p-type GaN grown by phase shift epitaxy

M. Zhong,[1] J. Roberts,[2] W. Kong,[3] A. S. Brown,[3] and A. J. Steckl[1,a)]
[1]*Department of Electrical Engineering and Computing Systems, University of Cincinnati, Cincinnati, Ohio 45221-0030, USA*
[2]*Nitronex Corporation, Raleigh, North Carolina 27606, USA*
[3]*Department of Electrical and Computer Engineering, Duke University, Durham, North Carolina 27708, USA*

(Received 21 June 2013; accepted 10 December 2013; published online 7 January 2014)

Phase shift epitaxy (PSE) is a periodic growth scheme, which desynchronizes host material growth process from dopant incorporation, allowing independent optimization. p-type doping of GaN with Mg by PSE is accomplished with molecular beam epitaxy by periodic shutter action (in order to iterate between Ga- and N-rich surface conditions) and by adjusting time delays between dopant and Ga shutters. Optimum PSE growth was obtained by turning on the Mg flux in the N-rich condition. This suppresses Mg self-compensation at high Mg concentration and produces fairly high hole concentrations ($2.4 \times 10^{18}\,cm^{-3}$). © *2014 AIP Publishing LLC*.
[http://dx.doi.org/10.1063/1.4861058]

Mg has a notoriously high activation energy {E_A(Mg)} of around 120–250 meV[1–3] in GaN, with an activation efficiency usually <10% at 25 °C. High hole concentration of $\sim 3 \times 10^{18}\,cm^{-3}$ has been demonstrated with MBE in both Ga-rich[4] and N-rich growth conditions.[5] Although significantly different growth conditions were used, the resulting films had similar Mg concentrations, limited to low $10^{19}\,cm^{-3}$ range in order to minimize Mg self-compensation or other defects. High Mg concentration is known to lead to defects due to the low solubility of Mg in Ga.[6] Mg self-compensation[7] and even GaN polarity inversion[8,9] are usually reported when higher Mg flux is used.

A dynamic MBE growth scheme—modulated metal epitaxy (MME)—has been reported[10] to promote Mg incorporation. During MME, the condition of the growth surface varies with a short period (5–10 s), with the shutters for the metal sources (Ga and dopants) opening and closing simultaneously, while the N shutter is continuously open. Hole concentration as high as $4.5 \times 10^{18}\,cm^{-3}$ with an accompanying mobility of 1.2 $cm^2/V{\cdot}s$ has been achieved with MME.[10] MME and other similar growth schemes,[11–14] such as metal enhanced epitaxy (MEE),[11] alternatively saturate the surface with Ga and N fluxes, so that good quality film is achieved even at relatively low growth temperatures.

Phase shift epitaxy (PSE) takes advantage of the variable surface conditions (specifically, Ga monolayer thickness) during dynamic growth to define a suitable time window for a selected dopant. The dopant shutter schedule is designed to be open during a specific period of time in each cycle so that the dopant is introduced only when the surface is either Ga-rich or N-rich. The timing sequences of different dynamic growth schemes[10,12,13] are shown in Fig. 1.

PSE doping of Eu in GaN under Ga-rich conditions has been previously reported[14] to yield a 10× enhancement of Eu luminescence efficiency. In this paper, high hole concentration in Mg-doped GaN is achieved by adjusting the PSE doping window to suppress Mg self-compensation at high Mg concentration.

Nitronex templates (with a 400 nm highly resistive GaN top layer on Si) were used in a Riber 32 MBE system. High purity N_2 (>6N) is used with an SVT 4.5 RF plasma source with ion removal control. The N_2 source condition (1.8 sccm, 230 W) produces a maximum growth rate of 0.72 ML/s using conventional (i.e., continuous) MBE growth conditions. A thermocouple attached to the back of the substrate holder indicates a temperature of 600 °C. During each cycle, the Ga shutter is open for 8 s to allow Ga to build up on surface and closed for the next 8 s to deplete the excess Ga atoms on the surface. The Mg shutter also opens for 8 s in each cycle, but is not synchronized with the Ga shutter. The Ga flux is kept at 9×10^{-7} Torr beam equivalent pressure (BEP) (equivalent to 1.1 ML/s), while the Mg flux is varied

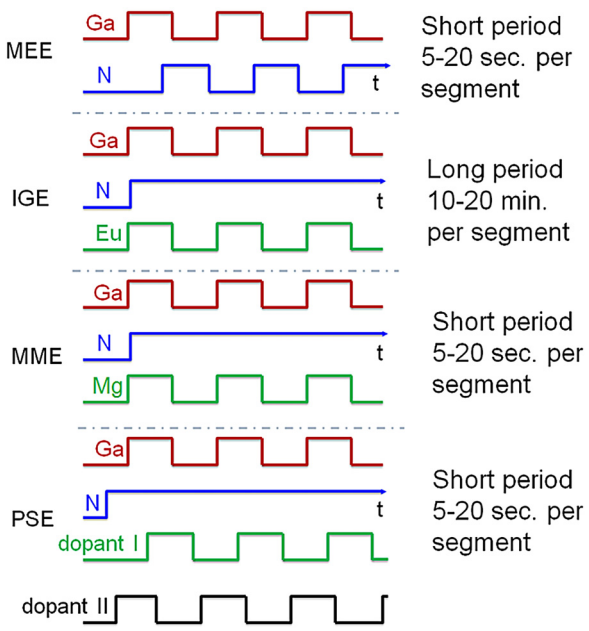

FIG. 1. Diagrams of Ga, N, and dopant fluxes vs. time in different modulated growth schemes. (Migration Enhanced Epitaxy, Interrupted Growth Epitaxy, Metal Migration Epitaxy, Phase Shift Epitaxy.)

a)Author to whom correspondence should be addressed. Electronic mail: a.steckl@uc.edu

from 2×10^{-10} to 3×10^{-9} Torr BEP. The overgrown film has a thickness of 450 nm after 50 min growth.

In order to determine the favorable surface condition for Mg doping, three sets of growth timing experiments (shown in Fig. 2) were performed. The PSE timing schedule is described by x/y//z/w, where "/" separates each segment in each period, "//" separates the Ga ON cycle and Ga OFF cycle and "_" is used to indicate that the Mg shutter is open during the segment.

Since PSE is a dynamic process, each metal beam requires a certain time for the surface coverage to reach maximum. The turn-on time is estimated using RHEED intensity variations.[15] The growth surface takes 2 s to change from N-rich to Ga-rich after the Ga shutter is open and for the reverse after the Ga shutter is closed. Since the variation of the Mg surface concentration cannot be directly observed, a model has been developed to simulate this process. The number of "free" Ga or Mg atoms on the surface has a changing rate equal to the incoming flux minus its consumption rate (by reaction with N) and loss by evaporation

$$\frac{dM_t}{dt} = F - G - D. \tag{1}$$

M_t is the metal layer thickness at time t in monolayers (ML), F is the incoming metal flux in ML/s, G is the growth rate or dopant incorporation rate in ML/s, and D is the desorption rate also in ML/s. G and D are further defined by "free" metal lifetimes: τ_1—before reacting with nitrogen, Eq. (1); τ_2—before evaporation (Eq. (2))

$$G(M_t, \tau_1) = \begin{cases} \frac{1}{\tau_1} \times M_t, & M_t < 1 \\ \frac{1}{\tau_1}, & M_t \geq 1, \end{cases} \tag{2}$$

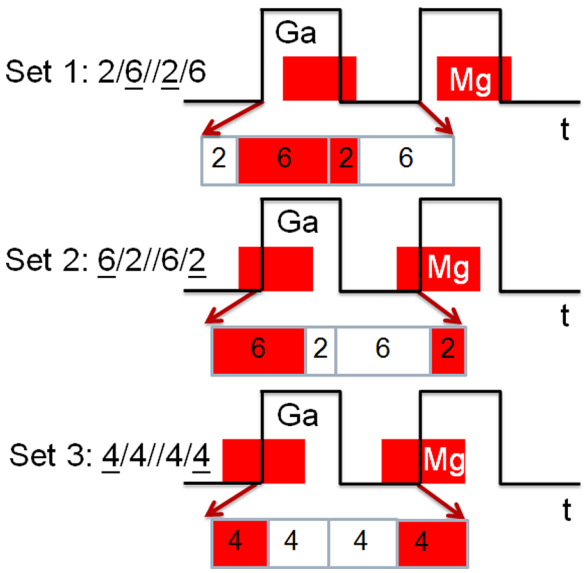

FIG. 2. Ga and Mg fluxes vs. time in PSE growth schemes for identification of optimum doping condition. "/" separates each segment in each period, "//" separates the Ga ON cycle and Ga OFF cycle and "_" is used to indicate that the Mg shutter is open during the segment.

$$D\frac{1}{\tau_2} \times M_t. \tag{3}$$

When the system reaches steady state in conventional MBE with a III/V of close to unity, $M_{Ga} = 1$ ML and $\frac{dM_{Ga}}{dt} = 0$ and $\frac{1}{\tau_2} \approx 0$ for Ga due to its low desorption rate at 600 °C. Thus, $\frac{1}{\tau_1}$ for Ga is estimated to be 0.72/s. For Mg

$$\frac{s}{1-s} = \frac{G_{Mg}}{D_{Mg}} = \frac{\frac{1}{\tau_1} \times M_{Mg}}{\frac{1}{\tau_2} \times M_{Mg}}, \tag{4}$$

where s is the Mg sticking coefficient, which changes with substrate temperature and surface condition. A rough estimation of the Mg sticking coefficient is 0.1, although some reports proposed a much lower number.[16] Since the growth is under kinetic limited condition, bonding is considered fast compared with mass transport and one can assume that Mg has the same incorporation rate G as Ga. Then $\frac{1}{\tau_2}$ for Mg can be estimated to be ~6.5/s. Solving the differential equation indicates that only ~0.2 s is required for Mg to reach 90% of its peak surface concentration and a similar amount of time is required to remove the Mg surface concentration. The Mg time constants will be larger with higher sticking coefficients, but still much smaller than those for Ga (~2–3 s). Hence, Mg can be considered to exhibit practically instant turn-on/off.

During growth, the surface starts with a streaky 1×1 RHEED pattern and changes to a slightly spotty pattern, as also observed by Namkoong *et al.*[17] The depth profile (Fig. 3) indicates fairly uniform doping throughout the overgrown GaN film (~400 nm thick). Although inversion domains[6] (IDs) with small density may exist in highly doped samples, no partial or total surface polarity inversion is found even at the highest Mg flux. The film polarity is indicated by the 2×2 RHEED pattern (Fig. 5 inset) during cooldown. The polarity was also checked with NaOH etching.[18] A droplet of saturated NaOH solution placed on the sample

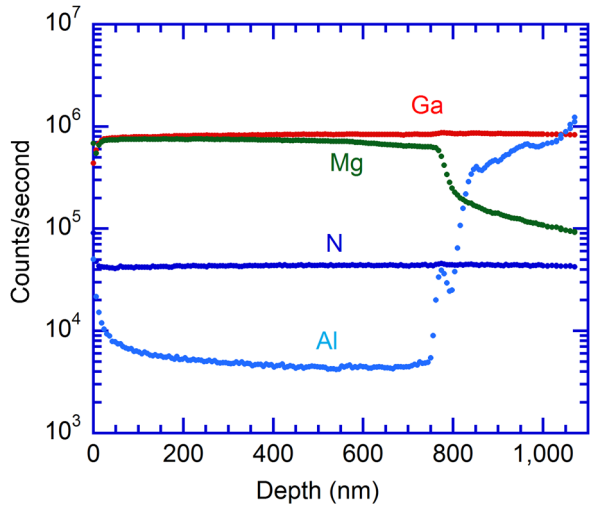

FIG. 3. SIMS depth profile for p type GaN doped with Mg (6/2//6/2). Mg flux used in this sample is 6×10^{-10} Torr BEP and Mg concentration is 4×10^{19} cm^{-3}.

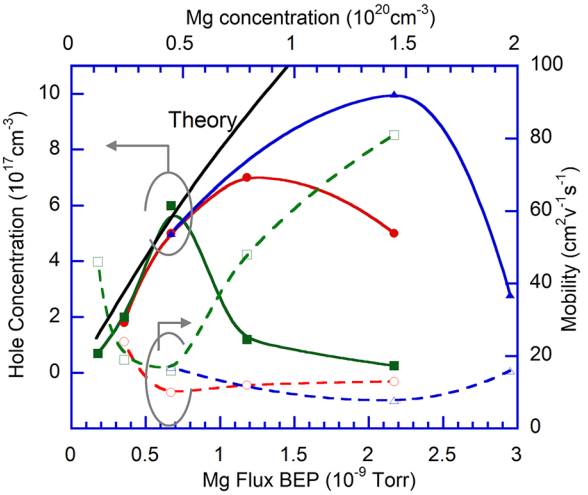

FIG. 4. Relationship between hole concentration/mobility and Mg flux/concentration for three sets of experiments (Set 1: ■□, Set 2: ●○, Set 3: ▲Δ). The solid lines connect the hole concentration data points (solid symbols). The dashed lines connect the mobility data points (open symbols).

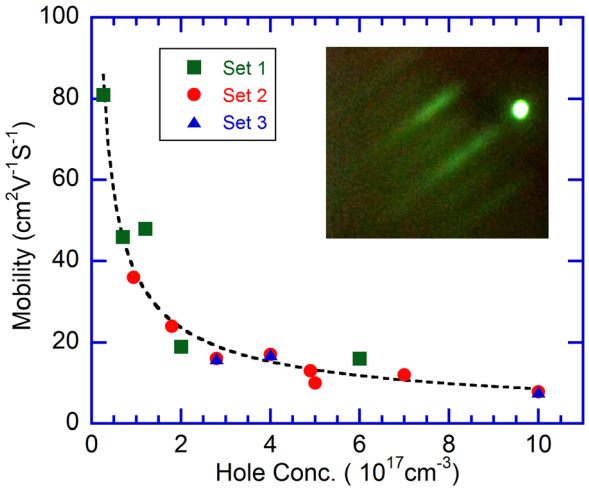

FIG. 5. Relationship between hole concentration and mobility for all samples in the three sets of experiments. Inset: RHEED 2 × 2 reconstruction during the cool down process after growth.

(20 min, 130 °C) produced no etching. Hall effect measurements from all three sets of experiments are shown in Fig. 4 as a function of Mg concentration. The data in the region where the hole concentration drops in each curve were repeated to confirm the trend. A theoretical curve of hole concentration vs. Mg concentration is shown based on background donor concentration of 3×10^{18} cm^{-3} and E_A(Mg) of 130 meV. The background donor concentration is obtained from an un-doped GaN sample. The E_A(Mg) is a best fit to the data and it falls in the range of reported values.[3,19]

In the low Mg flux region ($<5 \times 10^{19}$ cm^{-3}), the hole concentration curves for the three growth conditions are similar and agree well with the theoretical curve. However, as the Mg flux increases into the high 10^{19} and the 10^{20} cm^{-3} range, Set 1 samples experience a steep drop in hole concentration. The highest hole concentration at the turning point is 6×10^{17} cm^{-3} at a Mg concentration of 5×10^{19} cm^{-3}. The hole concentration of Set 2 peaks at 7×10^{17} cm^{-3}, produced by a Mg concentration of 8×10^{19} cm^{-3}. In Set 3, the Mg shutter opens for the longest time in the N-rich condition (low Ga ML thickness) of all three sets, and the peak hole concentration increases to 1×10^{18} cm^{-3} produced by a Mg concentration of 1.5×10^{20} cm^{-3}. All three sets experience a drop in hole concentration at higher Mg fluxes, probably due to Mg self-compensation effect. Doping in the N-rich condition clearly helps postpone the onset of hole concentration reduction at higher Mg flux levels.

Mg doping in an even more N-rich condition (3/5//5/3 and reduced Ga flux) resulted in the highest hole concentration of 2.4×10^{18} cm^{-3} obtained at a Mg flux BEP is 3.5×10^{-9} Torr.

The lowest resistivity among these samples is 0.5–0.7 Ω cm (Sets 1 and 2), while the highest hole concentration (Set 3) shows a resistivity of 1.0 Ω cm (because of lower mobility). The increase of resistivity when increasing Mg doping is due to introduction of defects. The overall relationship between the mobility and the hole concentration for all samples is plotted in Fig. 5. Data from all three sets follow a very similar trend, with the mobility monotonically decreasing with increasing hole concentration, in agreement with previous reports.[20]

Two samples (see Table I) with different growth schemes, but similar Mg concentrations, were selected for double crystal x-ray diffraction (XRD) analysis along with a template-only reference sample. Since the overgrown GaN PSE layer is somewhat thicker than the GaN layer in the template (450 nm vs. 400 nm), the signal from the PSE p-type layer can be distinguished. Representative XRD results are shown in Fig. 6 and summarized in Table I. Sample JT34 in Set 3 grown under N-rich conditions (growth scheme—4/4//4/4) exhibits narrower peaks than sample JT32 in Set 1 grown under Ga-rich conditions (2/6//2/6) in both (002) and (015) planes, indicating lower density of both screw and edge type dislocations. These results agree very well with the Hall effect measurements. Furthermore, in the case of sample JT34 the crystal quality indicated by the XRD represents an underestimate since some of the linewidth broadening is due to the underlying template.

GaN p-n junction diodes were fabricated in the following structure: p (5×10^{17} cm^{-3})/n (2×10^{17} cm^{-3})/n$^+$ (2×10^{18} cm^{-3}). The p-type layer was doped under PSE N-rich condition (8//5/3). Somewhat higher growth temperature was used to control the leakage current: 700 and 680 °C

TABLE I. Double X-Ray diffraction test result for selected samples.

Sample #	Growth scheme	Mg flux BEP (Torr)	Hole conc. (cm^{-3})	Mobility (cm^2/v-s)	FWHM (002) (arc sec)	FWHM (015) (arc sec)
JT32	2/6//2/6	2.2×10^{-9}	2.60×10^{16}	81	1206	979
JT34	4/4//4/4	2.2×10^{-9}	1.00×10^{18}	7.8	900	846
Template	NA	NA	NA	NA	1022	1098

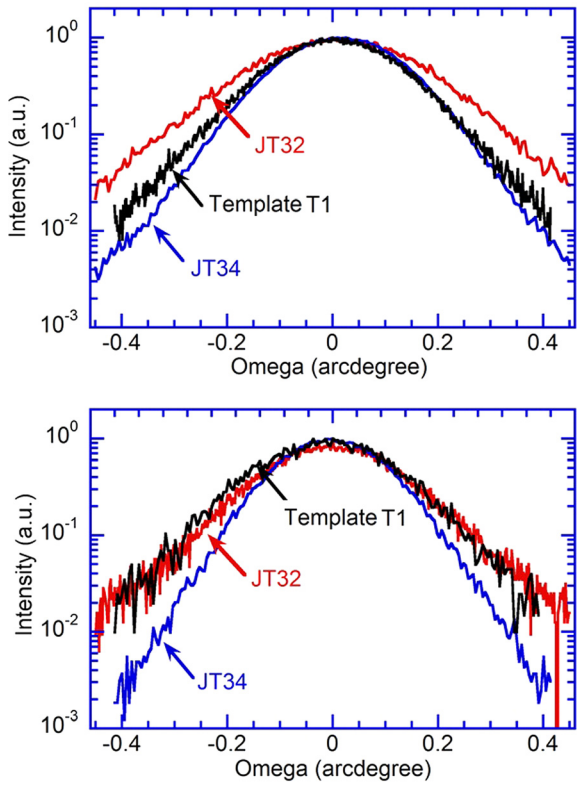

FIG. 6. Double Crystal X-Ray Diffraction results for JT34, JT32, and the template. Top: Peaks of (002) plane. Bottom: Peaks of (015) plane.

for n- and p-type layers, respectively. For the p-type layer growth, the Mg shutter is turned on for 3 s and then turned off before re-opening the Ga shutter. Thus, Mg is being doped completely in extreme N-rich condition. p-type surface polarity tested using NaOH etching method[18] showed no etching, indicating that no polarity inversion occurred during growth.

Fig. 7 shows the current-voltage characteristics of p-n junction diode fabricated by PSE. In this preliminary device demonstration, several non-ideal factors have limited the device performance. ITO and a large In pad were used as simple p- and n-type electrodes, resulting in high threshold voltage of 5 V and series resistance of $1\,\Omega\,cm^2$, compared with a published value[21] of $6.3\,m\Omega\ cm^2$. Furthermore, the high density of threading dislocations in the substrate results[22] in high leakage current and reduces the ON/OFF current ratio.

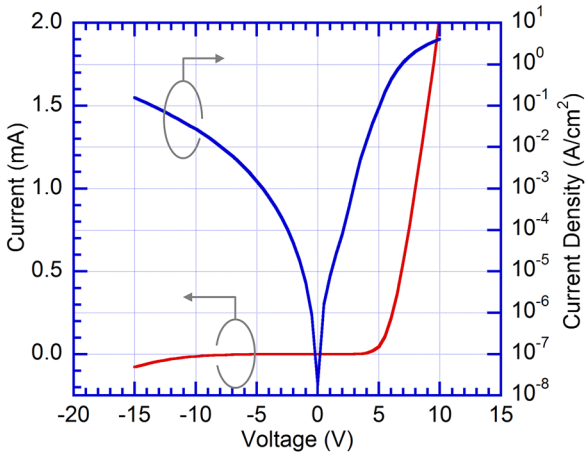

FIG. 7. Current-voltage characteristics for p-n GaN diode with p-type layer doping (Mg) in PSE extreme N-rich condition.

The manner in which dopants are incorporated into the lattice is strongly affected by the surface condition of the host material. During conventional MBE growth of GaN, ~1–2 liquid Ga monolayers exist on the surface. Mg incorporation into Ga sites is limited by the solubility of Mg in Ga. When complete solubility is not satisfied, excess Mg atoms tend to stay on the surface as surfactants[23] or to form defect structures such as IDs.[6] On the other hand, when Ga monolayer coverage is very low, Ga atoms and dopant atoms behave as separate individual species rather than liquids, so that complete solubility is not required. In addition, operating in the extreme N-rich condition significantly reduces adatom mobility so that Mg atoms are not likely to be incorporated jointly as self-compensating donors. The Ga-rich condition limits Mg incorporation, especially with high substrate temperature when Mg solubility in Ga is low. To the contrary, when most Mg is incorporated in a Ga-free environment, no noticeable polarity inversion is observed and higher hole concentration can be achieved with higher Mg concentration.

High Mg concentration (in the $10^{20}\,cm^{-3}$ range) has been reported[24,25] to help decrease E_A(Mg) in the GaN lattice in plasma enhanced MBE or gas source MBE, resulting in very high hole concentrations ($>10^{19}\,cm^{-3}$). In these cases, a dependence of the ionization energy with the Mg-acceptor concentration is found and explained by the formation of a broad defect band. This phenomenon was not observed in the experiments reported here even though the upper range of the Mg concentration was $2–3\times10^{20}\,cm^{-3}$. Possible causes for this phenomenon are the concentrations of impurities in the Mg source and the presence of damage-inducing species from the nitrogen plasma source.

The main features of PSE are: (1) ability to distinguish favorable surface condition for designated dopant related structure; (2) desynchronization between doping incorporation and host growth conditions, breaking the trade-off between optimum conditions for host growth and for doping. PSE could also be applied to the growth of alloy semiconductors, such as InGaN in which high In content can lead to non-uniformity of In distribution and the onset of clusters.

The research at Cincinnati was supported in part by a U.S. Army Research Office Grant (No. W911NF-10-1-0329).

[1]W. Gotz, N. M. Johnson, J. Walker, D. P. Bour, and R. A. Street, Appl. Phys. Lett. **68**(5), 667–669 (1996).
[2]J. W. Huang, T. F. Kuech, H. Q. Lu, and I. Bhat, Appl. Phys. Lett. **68**(17), 2392–2394 (1996).
[3]W. Kim, A. Salvador, A. E. Botchkarev, O. Aktas, S. N. Mohammad, and H. Morkoc, Appl. Phys. Lett. **69**(4), 559–561 (1996).
[4]A. Bhattacharyya, W. Li, J. Cabalu, T. D. Moustakas, D. J. Smith, and R. L. Hervig, Appl. Phys. Lett. **85**(21), 4956–4958 (2004).
[5]M. Zhang, P. Bhattacharya, W. Guo, and A. Banerjee, Appl. Phys. Lett. **96**(13), 132103 (2010).
[6]C. G. Van de Walle, C. Stampfl, and J. Neugebauer, J. Cryst. Growth **189–190**, 505–510 (1998).

[7]D. J. Dewsnip, J. W. Orton, D. E. Lacklison, L. Flannery, A. V. Andrianov, I. Harrison, S. E. Hooper, T. S. Cheng, C. T. Foxon, S. N. Novikov, B. Y. Ber, and Y. A. Kudriavtsev, Semicond. Sci. Technol. **13**(8), 927–935 (1998).
[8]S. Pezzagna, P. Vennéguès, N. Grandjean, and J. Massies, J. Cryst. Growth **269**(2–4), 249–256 (2004).
[9]V. Ramachandran, R. M. Feenstra, W. L. Sarney, L. Salamanca-Riba, J. E. Northrup, L. T. Romano, and D. W. Greve, Appl. Phys. Lett. **75**(6), 808–810 (1999).
[10]S. D. Burnham, G. Namkoong, D. C. Look, B. Clafin, and W. A. Doolittle, J. Appl. Phys. **104**(2), 024902 (2008).
[11]Y. Homma, H. Yamaguchi, and Y. Horikoshi, Appl. Phys. Lett. **68**(1), 63–65 (1996).
[12]Y. Y. Wong, E. Y. Chang, Y. H. Wu, M. K. Hudait, T. H. Yang, J. R. Chang, J. T. Ku, W. C. Chou, C. Y. Chen, J. S. Maa, and Y. C. Lin, Thin Solid Films **519**(19), 6208–6213 (2011).
[13]C. Munasinghe and A. J. Steckl, Thin Solid Films **496**(2), 636–642 (2006).
[14]M. Y. Zhong and A. J. Steckl, Appl. Phys. Express **3**(12), 121002 (2010).
[15]M. Moseley, D. Billingsley, W. Henderson, E. Trybus, and W. A. Doolittle, J. Appl. Phys. **106**(1), 014905–014907 (2009).
[16]S. D. Burnham, "Improved understanding and control of magnesium doped gallium nitride by plasma assisted molecular beam epitaxy," Ph.D. thesis, Georgia Institute of Technology, Atlanta, 2007.
[17]G. Namkoong, E. Trybus, K. K. Lee, M. Moseley, W. A. Doolittle, and D. C. Look, Appl. Phys. Lett. **93**(17), 172112–172113 (2008).
[18]A. R. Smith, R. M. Feenstra, D. W. Greve, M. S. Shin, M. Skowronski, J. Neugebauer, and J. E. Northrup, Appl. Phys. Lett. **72**(17), 2114–2116 (1998).
[19]J. Kim, D. Y. Ryu, N. A. Bojarczuk, J. Karasinski, S. Guha, S. H. Lee, and J. H. Lee, J. Appl. Phys. **88**(5), 2564–2569 (2000).
[20]U. Kaufmann, P. Schlotter, H. Obloh, K. Kohler, and M. Maier, Phys. Rev. B **62**(16), 10867–10872 (2000).
[21]T. Tanabe, S. Hashimoto, Y. Yoshizumi, and M. Kiyama, SEI Tech. Rev. **64**(21), 21–26 (2007).
[22]S. W. Lee, D. C. Oh, H. Goto, J. S. Ha, H. J. Lee, T. Hanada, M. W. Cho, T. Yao, S. K. Hong, H. Y. Lee, S. R. Cho, J. W. Choi, J. H. Choi, J. H. Jang, J. E. Shin, and J. S. Lee, Appl. Phys. Lett. **89**(13), 132117 (2006).
[23]E. Monroy, T. Andreev, P. Holliger, E. Bellet-Amalric, T. Shibata, M. Tanaka, and B. Daudin, Appl. Phys. Lett. **84**(14), 2554–2556 (2004).
[24]S. Brochen, J. Brault, S. Chenot, A. Dussaigne, M. Leroux, and B. Damilano, Appl. Phys. Lett. **103**(3), 032102 (2013).
[25]B. Gunning, J. Lowder, M. Moseley, and W. A. Doolittle, Appl. Phys. Lett. **101**(8), 082106 (2012).